# PACIAE 2.0: An updated parton and hadron cascade model (program) for the relativistic nuclear collisions

Ben-Hao Sa,[1, 2, 3, *] Dai-Mei Zhou,[2] Yu-Liang Yan,[1] Xiao-Mei Li,[1] Sheng-Qin Feng,[4] Bao-Guo Dong,[1] and Xu Cai[2]

[1]*China Institute of Atomic Energy, P. O. Box 275 (18), Beijing, 102413 China*
[2]*Institute of Particle Physics, Huazhong Normal University, Wuhan, 430082 China*
[3]*CCAST (World Lab.), P. O. Box 8730 Beijing, 100080 China*
[4]*Department of Physics, College of Science, Three Gorges University, Yichang, 443002 China*

We have updated the parton and hadron cascade model PACIAE for the relativistic nuclear collisions, from based on JETSET 6.4 and PYTHIA 5.7 to based on PYTHIA 6.4, and renamed as PACIAE 2.0. The main physics concerning the stages of the parton initiation, parton rescattering, hadronization, and hadron rescattering were discussed. The structures of the programs were briefly explained. In addition, some calculated examples were compared with the experimental data. It turns out that this model (program) works well.

## PROGRAM SUMMARY

*Title of program:* PACIAE version 2.0
*Catalogue number:* ADBS
*Program obtained from:* CPC Program Library, Queen's University, Belfast, N. Ireland; or from yanyl@ciae.ac.cn, zhoudm@phy.ccnu.edu.cn, sabh@ciae.ac.cn
*Computer for which the program is designed and others on which it has been tested:* DELL Studio XPS and others with a FORTRAN 77 or GFORTRAN compiler
*Computer:* DELL Studio XPS
*Programming languages:* FORTRAN 77
*Memory required to execute with typical data:* ≈1G words
*No. of bits in a word:* 64
*Peripherals used:* terminal for input, terminal or printer for output
*No. of lines in distributed program, including test data, etc.:* ≈200000
*Distribution format:* tar.gz
*Nature of physical problem:* The Monte Carlo simulation of hadron transport (cascade) model is successful in studying the observables at final state in the relativistic nuclear collisions. However the high $p_T$ suppression, the jet quenching (energy loss), and the eccentricity scaling of $v_2$ etc., observed in high energy nuclear collisions, indicates the important effect of the initial partonic state on the final hadronic state. Therefore the better parton and hadron transport (cascade) models for the relativistic nuclear collisions are highly required.
*Method of solution:* The parton and hadron cascade model PACIAE is originally based on the JETSET 7.4 and PYTHIA 5.7. The PYTHIA model has been updated to PYTHIA 6.4 with the additions of new physics, the improvements in existing physics, and the embedding of the JETSET model etc.. Therefore we update the PACIAE model to the new version of PACIAE 2.0 based on the PYTHIA 6.4 in this paper. In addition, some improvements in physics have been introduced in this new version.
*Restrictions:* Depend on the problem studied.
*Typical running time:* Depend on the type of collision and energy. Examples running on the DELL Studio XPS are follows:

- Running 1000 events for inelastic pp collisions at $\sqrt{s}$=200 GeV by program PACIAE 2.0a to reproduce PHOBOS data of rapidity density at mid-rapidity, $dN_{ch}/dy$=$2.25^{+0.37}_{-0.30}$ [1], spends ≈ 3 minutes.

- Running 0-6% most central Au+Au collision at $\sqrt{s_{NN}}$=200 GeV by program PACIAE 2.0b and PACIAE 2.0c to reproduce PHOBOS data of charged multiplicity of 5060 [2] spends ≈13 seconds/event and ≈265 seconds/event, respectively.

*PACS:* 25.75.Dw, 24.10.Lx
*Keywords:* relativistic nuclear collision; transport (cascade) model; hadron; parton; parton rescattering; hadronization; hadron rescattering.

---

*Electronic address: sabh@ciae.ac.cn

# LONG WRITE-UP

## I. INTRODUCTION

The hadron transport (cascade) model is successful in describing the relativistic nuclear collisions. However, many new phenomena observed in the relativistic nucleus-nucleus (including proton-nucleus) collisions at RHIC energies, such as high $p_T$ suppression [3, 4], jet quenching (energy loss) [5], and elliptic flow eccentricity scaling [6] etc., strongly indicate the important effect of the partonic initial state on the hadronic final state. The better parton and hadron transport (cascade) model is urgently required.

The first parton and hadron cascade model [7] encouraged copious publications of the similar models, such as AMPT (string melting) [8], PACIAE [9], BAMPS (parton cascade only) [10], PHSD [11], and MARTINI [12] etc.. Among them the PACIAE model, a parton and hadron cascade model for relativistic nuclear collision, is based on PYTHIA 5.7 and JETSET 7.4 [13]. We have employed this PACIAE model successfully studying [14]:

- limiting fragmentation phenomenon in elementary and heavy-ion collisions,

- fluctuations and correlations in particle production,

- direct photon production in pp and Au+Au collisions at RHIC energies,

- property of QCD matter at RHIC and LHC energies,

- charged particle and strange particle productions in pp collisions at LHC energies,

- charged particle elliptic flow in pp collisions at LHC energies.

In this paper, the PACIAE model is updated to PACIAE 2.0 based on PYTHIA 6.4 [15] with the additions of new physics and the improvements in existing physics. As the latest version PYTHIA 8.1 [16] "does not yet in every respect replaces the old code" and the physical differences between PYTHIA 8.1 and PYTHIA 6.4 are not important for the investigation of nucleus-nucleus collisions, so we left the connection with PYTHIA 8.1 in the future.

PYTHIA 6.4 is a Monte Carlo event generator for relativistic hadron-hadron collisions in hadronic level. In this model a pp (hadron-hadron, hh) collision is decomposed into parton-parton collisions. A hard parton-parton collision is described by the lowest leading order perturbative QCD (LO-pQCD). The soft parton-parton collision, non-perturbative phenomenon, is considered empirically. Because the initial- and final-state QCD radiations and multiparton interactions are considered in the parton-parton scattering, the consequence of a hh collision is a parton multijet configuration composed of di-quarks (anti-diquarks), quarks (anti-quarks), and gluons, besides a few hadronic remnants. This parton multijet configuration is followed by the string construction and fragmentation (hadronization). Therefore one obtains a hadronic final state for a hh (pp) collision. If one switches off the string fragmentation and breaks up the di-quarks (anti-diquarks) to quarks (anti-quarks), one then obtains a state composed of the quarks, anti-quarks, and the gluons. This is the key point in the creation of the parton and hadron cascade model PACIAE for the relativistic nuclear collisions.

The PACIAE model composes of four stages of the parton initiation, parton rescattering, hadronization, and hadron rescattering. PACIAE 2.0 has three versions: PACIAE 2.0a describing the relativistic pp collision ($\bar{p}p$, or $e^+e^-$, denoted as elementary collision later) and PACIAE 2.0b as well as PACIAE 2.0c describing the relativistic nucleus-nucleus (A+B, including p+A) collisions. The hybrid system of units, based on the mass in GeV, length in fm, and time in fm with $c=1$ and $hc=1.24$ GeV·fm, is used in PACIAE 2.0.

The rest of this paper is organized as follows: Section II discussed the main physics in the PACIAE model except the ones in PYTHIA:

- nucleon initiation in the position and momentum phase spaces,

- particle propagation (cascade) and the collision criteria,

- cross sections,

- determination of the scattered particles,

- diquark break-up,

- reduction of the strange (heavy) quark suppression,

- deexcitation of the energetic quark (antiquark) in the coalescence model.

We explain the structures of programs in section III. The examples are calculated and compared with the experimental data in section IV. We give the users' guide in the appendix.

## II. PHYSICS CONCERNED

The PYTHIA 6.4 model involves abundant particle and nuclear physics contents which have been discussed in [15] in the detail. Here we just introduce the extra physics concerned with the nuclear initiation, the parton rescattering, and the hadron rescattering.

### A. Nucleon initiation in the position and momentum phase spaces

#### 1. Impact parameter and its sampling

In the experiments the centrality bins are defined by the cuts in the particle multiplicity distribution and indicated by the percentages, $g$, in the geometric (total) cross section. However, the centrality is conveniently defined theoretically by the impact parameter $b$. A mapping relation between $g$ and $b$

$$b = \sqrt{g}b_{max}, b_{max} = R_A + R_B \tag{1}$$

was introduced according to the definition of geometric cross section [17].

As the experiments of nucleus-nucleus collisions are always performed in a given centrality bin the relevant theoretical calculations should span the corresponding impact parameter interval from $b_d$ to $b_u$. We sample impact parameter $b_i$ randomly by

$$b_i = \sqrt{\xi \times (b_u^2 - b_d^2) + b_d^2}, \tag{2}$$

and generate a nucleus-nucleus collision event. In the above equation $\xi$ refers to a random number. The observable (operator) averaged over the events generated by different $b_i$ (i=1,2,...) can compare with the corresponding experimental data.

One may also use the systematic sampling method:

$$\int_{b_0=b_d}^{b_1} bdb = \int_{b_1}^{b_2} bdb = ... = \int_{b_{n-1}}^{b_n=b_u} bdb = \frac{b_u^2 - b_d^2}{2n}, \tag{3}$$

$$b_j = \sqrt{j\frac{b_u^2 - b_d^2}{n} + b_d^2}, \qquad j = 0, 1, 2, ..., n \ (n \ even) \tag{4}$$

The set of $b_j(j = 1, 3, 5, ..., n-1)$ is then the sampled spectral values. We generate events by these spectral values repeatedly and compare the event averaged observable with the corresponding experimental data.

#### 2. Geometric overlap zone and number of participant nucleons

For a nucleus-nucleus collision A+B at a given impact parameter $b$, a geometric overlap zone is formed between colliding nuclei in the position phase space. The nucleons located inside this zone are the participant nucleons, otherwise the spectator nucleons. The geometric number of participant nucleons is calculated [17] by

$$N_{part}(b) = N_{part}^A(b) + N_{part}^B(b), \tag{5}$$

$$N_{part}^A(b) = \rho_A \int dV \theta(R_A - (x^2 + (b-y)^2 + z^2)^{1/2})\theta(R_B - (x^2 + y^2)^{1/2}), \tag{6}$$

$$N_{part}^B(b) = \rho_B \int dV \theta(R_B - (x^2 + y^2 + z^2)^{1/2})\theta(R_A - (x^2 + (b-y)^2)^{1/2}), \tag{7}$$

where

$$\theta(x) = \begin{cases} 0 & if \ \ x < 0 \\ 1 & otherwise \end{cases} \tag{8}$$

$R_A$ and $\rho_A$ ($R_B$ and $\rho_B$) are the radius and nuclear density of the nucleus $A$ ($B$), respectively. The nuclear density of nucleus $A$ is normalized to the atomic number $A$ (we denote the nucleus and its atomic number by $A$ uniquely). The STAR and PHOBOS collaborations have reported that their analysed Glauber model number of participant nucleons is nearly reaction energy independent for a given centrality A+B collisions within error bars [1, 18]. Therefore we assume normal nuclear density of $\rho_A = \rho_B = \rho_0$=0.16 fm$^{-3}$ here.

The geometric number of spectator nucleons is then calculated by

$$N^A_{spec} = A - N^A_{part}, \ \ N^B_{spec} = B - N^B_{part}. \tag{9}$$

### 3.   Nucleon initiation in the position and momentum phase spaces

The geometric participant nucleons in each of the colliding nuclei are distributed randomly inside the geometric overlap zone. And the geometric spectator nucleons are distributed according to the Woods-Saxon distribution and $4\pi$ uniform distribution and requiring to be outside the geometric overlap zone. These distrbutions are

$$\rho(r) = \rho_0(1 + \exp\frac{r - R}{d})^{-1}, \tag{10}$$

$$f(\theta, \phi) = \frac{1}{4\pi}, \tag{11}$$

where $R = r_0 A^{1/3}$+0.54 fm is the radius of nucleus $A$, the stander root-mean-square-radius parameter $r_0 \sim$1.15 fm, and $d \sim 0.54$ fm is the length of diffusion tail.

For the case of collider the $x$ and $y$ components of momentum of each nucleons in colliding nucleus are assumed to be zero, provided the beam is orientated towards the $z$ direction. The beam momentum is given to $p_z$ for each nucleons properly. This means the effect of Fermi motion is neglected in the relativistic nuclear collisions.

## B.   Particle propagation (cascade) and the collision criteria

The particles (partons in the parton rescattering stage or hadrons in the hadron rescattering stage) are assumed to travel in the straight trajectories

$$\vec{r}_i = \vec{R}_i + \vec{\beta}_i(t - T_i) \tag{12}$$

along the momentum direction during two consecutive collisions. In the above equation ($\vec{R}_i$, $T_i$) and $\vec{\beta}_i$ stand for the four-position and velocity of the $i$-th particle at the moment of last collision, respectively.

The particles interact with each other by means of total cross section. In order to perform the collisions in a consistent way one needs to introduce a time ordering procedure. We calculate the time between the last and the next possible collisions for all particle pairs and then choose the minimum collision time pair to perform the particle-particle collision [19]. A particle-particle collision (particle $i$ bombards with $j$, for instance) is defined to occur provided the minimum approaching distance ($D$) between particles $i$ and $j$, in their cms system, satisfies [19]

$$D \le \sqrt{\sigma_{tot}/\pi}, \tag{13}$$

where $\sigma_{tot}$ is the total cross section in fm$^2$. We calculate $D$ starting from the trajectories of particle $i$ and $j$ in their cms system (variables in the cms system indicated with superscript $*$)

$$\vec{r}^*_i = \vec{R}^*_i + \vec{\beta}^*_i(t^* - T^*_i) \ \ , \ \ \vec{r}^*_j = \vec{R}^*_j + \vec{\beta}^*_j(t^* - T^*_j). \tag{14}$$

The squared relative distance between $i$ and $j$ reads

$$d^2(t^*) = (\Delta\vec{R}^*)^2 + 2\Delta\vec{R}^*\Delta\vec{\beta}^*[t^* - \frac{1}{\Delta\vec{\beta}^*}(\vec{\beta}^*_j T^*_j - \vec{\beta}^*_i T^*_i)] + (\Delta\vec{\beta}^*)^2[t^* - \frac{1}{\Delta\vec{\beta}^*}(\vec{\beta}^*_j T^*_j - \vec{\beta}^*_i T^*_i)]^2, \tag{15}$$

where

$$\Delta\vec{R}^* = \vec{R}_j^* - \vec{R}_i^*, \quad \Delta\vec{\beta}^* = \vec{\beta}_j^* - \vec{\beta}_i^*. \tag{16}$$

From the requirement of

$$\frac{\partial(d^2(t^*))}{\partial t^*} = 0 \tag{17}$$

one obtains the collision time at the moment of $i$ bombarding with $j$

$$t_{ij}^* = \frac{-\Delta\vec{R}^*\Delta\vec{\beta}^* + \Delta\vec{\beta}^*(\vec{\beta}_j^* T_j^* - \vec{\beta}_i^* T_i^*)}{(\Delta\vec{\beta}^*)^2}. \tag{18}$$

Inserting Eq. (18) into Eq. (15), the corresponding minimum approaching distance is obtained

$$D = [(\Delta\vec{R}^*)^2 + \Delta\vec{R}^*\Delta\vec{\beta}^*(t_{ij}^* - \frac{1}{\Delta\vec{\beta}^*}(\vec{\beta}_j^* T_j^* - \vec{\beta}_i^* T_i^*))]^{1/2}. \tag{19}$$

As the particle collision must be causal, the above calculated collision time should satisfy

$$t_{ij}^* \geq \max(T_i^*, T_j^*). \tag{20}$$

Eqs. (13) and (20) are the criteria for a particle-particle collision to occur.

This collision time has to boost back from the cms of colliding pair to the cms of nucleus-nucleus collision according to the inverse Lorentz transformation [20, 21]

$$\begin{aligned}
\vec{r} &= \vec{r^*} + \vec{\beta}[\frac{(\gamma-1)\vec{r^*}\cdot\vec{\beta}}{\beta^2} + \gamma t^*], \\
t &= \gamma(t^* + \vec{r^*}\cdot\vec{\beta}), \\
\vec{\beta} &= \frac{\vec{p}_i + \vec{p}_j}{E_i + E_j}, \\
\gamma &= \frac{1}{\sqrt{1-\beta^2}},
\end{aligned} \tag{21}$$

where $\vec{\beta}$ refers to the velocity of cms of colliding pair in the frame of the cms of nucleus-nucleus collision. Ordering the collision times calculated for all collision pairs, the collision (time) list is obtained.

The corresponding Lorentz transformation reads [20, 21]

$$\vec{r^*} = \vec{r} + \vec{\beta}[\frac{(\gamma-1)\vec{r}\cdot\vec{\beta}}{\beta^2} - \gamma t],$$

$$t^* = \gamma(t - \vec{r}\cdot\vec{\beta}). \tag{22}$$

Replacing four position $(\vec{r}, t)$ with four momentum $(\vec{p}, E)$ in Eq. (22) and (21) one obtains, respectively, the Lorentz transformation and inverse Lorentz transformation for the four momentum.

### C. Cross sections

#### 1. Hadron-hadron cross sections

The isospin averaged parametrization formulas are employed for the hh cross sections [22, 23]. Taking the $\pi + p \to k + Y$ ($Y$ refers to $\Lambda$ and $\Sigma$) reactions as example, the cross sections are
$\pi^+ p \to \Sigma^+ k^+$:

$$\sigma(\sqrt{s}) = \begin{cases}
A_1(\sqrt{s}-1.683), & 1.683 \text{ GeV} < \sqrt{s} < 1.934 \text{ GeV}, \\
\qquad A_1 = 0.7 \text{ mb}/0.218 \text{ GeV}, \\
A_2 \exp(-A_3\sqrt{s}), & 1.934 \text{ GeV} < \sqrt{s} < 3.0 \text{ GeV}, \\
\qquad A_2 = 60.26 \text{ mb}, \quad A_3 = 2.31 \text{ GeV}^{-1}, \\
A_4 \exp(-A_5\sqrt{s}), & 3.0 \text{ GeV} < \sqrt{s}, \\
\qquad A_4 = 0.36 \text{ mb}, \quad A_5 = 0.605 \text{ GeV}^{-1},
\end{cases} \tag{23}$$

$\pi^- p \to \Lambda k^0$:

$$\sigma(\sqrt{s}) = \begin{cases} A_1(\sqrt{s} - 1.613), & 1.613 \text{ GeV} < \sqrt{s} < 1.684 \text{ GeV}, \\ & A_1 = 0.9 \text{ mb}/0.091 \text{ GeV}, \\ A_2 \exp(-A_3\sqrt{s}), & 1.684 \text{ GeV} < \sqrt{s} < 2.1 \text{ GeV}, \\ & A_2 = 436.3 \text{ mb}, \quad A_3 = 4.154 \text{ GeV}^{-1}, \\ A_4 \exp(-A_5\sqrt{s}), & 2.1 \text{ GeV} < \sqrt{s}, \\ & A_4 = 0.314 \text{ mb}, \quad A_5 = 0.301 \text{ GeV}^{-1}, \end{cases} \tag{24}$$

$\pi^- p \to \Sigma^0 k^0$:

$$\sigma(\sqrt{s}) = \begin{cases} A_1(\sqrt{s} - 1.689), & 1.689 \text{ GeV} < \sqrt{s} < 1.722 \text{ GeV}, \\ & A_1 = 10.6 \text{ mb/ GeV}, \\ A_2 \exp(-A_3\sqrt{s}), & 1.722 \text{ GeV} < \sqrt{s} < 3.0 \text{ GeV}, \\ & A_2 = 13.7 \text{ mb}, \quad A_3 = 1.92 \text{ GeV}^{-1}, \\ A_4 \exp(-A_5\sqrt{s}), & 3.0 \text{ GeV} < \sqrt{s}, \\ & A_4 = 0.188 \text{ mb}, \quad A_5 = 0.611 \text{ GeV}^{-1}, \end{cases} \tag{25}$$

$\pi^- p \to \Sigma^- k^+$:

$$\sigma(\sqrt{s}) = \begin{cases} A_6(constant), & 1.691 \text{ GeV} < \sqrt{s} < 1.9 \text{ GeV}, \\ A_4 \exp(-A_5\sqrt{s}), & 1.9 \text{ GeV} < \sqrt{s}, \\ & A_4 = 309.06 \text{ mb}, \quad A_5 = 3.77 \text{ GeV}^{-1}. \end{cases} \tag{26}$$

An assumed constant total cross sections of $\sigma_{\text{tot}}^{NN} = 40$ mb (RHIC energy region) or 76 mb (LHC energy region) [21], $\sigma_{\text{tot}}^{\pi N} = 25$ mb, $\sigma_{\text{tot}}^{kN} = 21$ mb, and $\sigma_{\text{tot}}^{\pi\pi} = 10$ mb as well as the inelastic to total cross section ratio of 0.85 are provided as another option. We assume

$$\sigma_{tot}^{pp} = \sigma_{tot}^{nn} = \sigma_{tot}^{pn} = \sigma_{tot}^{\Delta n} = \sigma_{tot}^{\Delta\Delta}. \tag{27}$$

The above hh cross sections are used in the hadron rescattering stage and in the parton initiation stage for the nucleus-nucleus collisions as well.

## 2. Parton-parton cross sections

We consider only the $2 \to 2$ parton-parton (re)scattering at the moment. The nine parton-parton differential cross sections calculated by means of LO-pQCD [24, 25] are:

$$\frac{d\hat{\sigma}}{d\hat{t}}(ab \to cd; \hat{s}, \hat{t}) = \frac{\pi\alpha_s^2}{\hat{s}^2}|\overline{M}(ab \to cd)|^2, \tag{28}$$

$$|\overline{M}(q_iq_j \to q_iq_j)|^2 = \frac{4}{9}\frac{\hat{s}^2 + \hat{u}^2}{\hat{t}^2} \approx \frac{8}{9}\frac{\hat{s}^2}{\hat{t}^2}, \tag{29}$$

$$|\overline{M}(q_iq_i \to q_iq_i)|^2 = \frac{4}{9}\left(\frac{\hat{s}^2 + \hat{u}^2}{\hat{t}^2} + \frac{\hat{s}^2 + \hat{t}^2}{\hat{u}^2}\right) - \frac{8}{27}\frac{\hat{s}^2}{\hat{u}\hat{t}} \approx \frac{8}{9}\frac{\hat{s}^2}{\hat{t}^2}, \tag{30}$$

$$|\overline{M}(q_i\bar{q}_j \to q_i\bar{q}_j)|^2 = \frac{4}{9}\frac{\hat{s}^2 + \hat{u}^2}{\hat{t}^2} \approx \frac{8}{9}\frac{\hat{s}^2}{\hat{t}^2}, \tag{31}$$

$$|\overline{M}(q_i\bar{q}_i \to q_j\bar{q}_j)|^2 = \frac{4}{9}\frac{\hat{t}^2 + \hat{u}^2}{\hat{s}^2} \approx 0, \tag{32}$$

$$|\overline{M}(q_i\bar{q}_i \to q_i\bar{q}_i)|^2 = \frac{4}{9}\left(\frac{\hat{s}^2 + \hat{u}^2}{\hat{t}^2} + \frac{\hat{t}^2 + \hat{u}^2}{\hat{s}^2}\right) - \frac{8}{27}\frac{\hat{u}^2}{\hat{s}\hat{t}} \approx \frac{8}{9}\frac{\hat{s}^2}{\hat{t}^2}, \tag{33}$$

$$|\overline{M}(q_i\bar{q}_i \to gg)|^2 = \frac{32}{27}\frac{\hat{u}^2 + \hat{t}^2}{\hat{u}\hat{t}} - \frac{8}{3}\frac{\hat{u}^2 + \hat{t}^2}{\hat{s}^2} \approx -\frac{32}{27}\frac{\hat{s}}{\hat{t}}, \tag{34}$$

$$|\overline{M}(gg \to q_i\bar{q}_i)|^2 = \frac{1}{6}\frac{\hat{u}^2 + \hat{t}^2}{\hat{u}\hat{t}} - \frac{3}{8}\frac{\hat{u}^2 + \hat{t}^2}{\hat{s}^2} \approx -\frac{1}{3}\frac{\hat{s}}{\hat{t}}, \tag{35}$$

$$|\overline{M}(q_ig \to q_ig)|^2 = -\frac{4}{9}\frac{\hat{u}^2 + \hat{s}^2}{\hat{u}\hat{s}} + \frac{\hat{u}^2 + \hat{s}^2}{\hat{t}^2} \approx \frac{2\hat{s}^2}{\hat{t}^2}, \tag{36}$$

$$|\overline{M}(gg \to gg)|^2 = \frac{9}{2}\left(3 - \frac{\hat{u}\hat{t}}{\hat{s}^2} - \frac{\hat{u}\hat{s}}{\hat{t}^2} - \frac{\hat{s}\hat{t}}{\hat{u}^2}\right) \approx \frac{9}{2}\frac{\hat{s}^2}{\hat{t}^2}. \tag{37}$$

Here the parton is represented as a classical point-like particle and specified by its internal degree of freedoms: flavor, rest (current) mass, momentum, and position. The spin and color degrees of freedoms are not explicitly included [7]. Therefore the amplitudes $|\overline{M}|^2$ are calculated by averaging over spin and color degrees of freedoms. The parton energy is determined by $E^2 = p^2 + m^2 + M^2$, where $M$ refers to virtual mass ($M^2=0$ for on mass shell parton, $M^2 <0$ for space-like parton, and $M^2 >0$ for time-like parton) [7]. $\alpha_s$ refers to the effective strong coupling constant. $\hat{s}$, $\hat{t}$, and $\hat{u}$ stand for the Mandelstam variables. In each of the above equations the second form is obtained by keeping only the leading divergent terms [26] with the assumption of the parton current mass is negligible relative to the cms energy. This assumption leads to

$$\hat{s} + \hat{t} + \hat{u} = 0. \tag{38}$$

The subprocesses of Eqs. (32), (34), and (35) are inelastic (re)scatterings, otherwise elastic. Subprocess of Eq. (32) is always negligible.

If the thermal direct photon is interested following two subprocesses have to be included:

$$|\overline{M}(q\bar{q} \to g\gamma)|^2 = \frac{8}{9}\frac{\alpha}{\alpha_s}e_q^2\left(\frac{\hat{u}}{\hat{t}} + \frac{\hat{t}}{\hat{u}}\right) \approx -\frac{16}{9}\frac{\alpha}{\alpha_s}e_q^2\frac{\hat{s}}{\hat{t}}, \tag{39}$$

$$|\overline{M}(qg \to q\gamma)|^2 = -\frac{1}{3}\frac{\alpha}{\alpha_s}e_q^2\left(\frac{\hat{t}}{\hat{s}} + \frac{\hat{s}}{\hat{t}}\right) \approx -\frac{1}{3}\frac{\alpha}{\alpha_s}e_q^2\frac{\hat{s}}{\hat{t}}, \tag{40}$$

where $\alpha=1/137$ stands for the fine-structure constant, $e_q$ refers to the charge of quark $q$.

## D. Determination of the scattered particles

The particle-particle (re)scattering is always dealt in the cms of colliding pair. The superscript $*$ is neglected in the rest of this section, except mentioned specially.

### 1. Hadron-hadron collisions

For an inelastic hadron (re)scattering $1 + 2 \to 3 + 4$ ($m_1 \neq m_3, m_2 \neq m_4$), the four momentum of the scattered particle reads

$$
\begin{aligned}
|\vec{p}_3|^2 = |\vec{p}_4|^2 &= \frac{[s - (m_3 + m_4)^2][s - (m_3 - m_4)^2]}{4s}, \\
\epsilon_3 &= \frac{s + (m_3^2 - m_4^2)}{2\sqrt{s}}, \\
\epsilon_4 &= \frac{s - (m_3^2 - m_4^2)}{2\sqrt{s}}.
\end{aligned}
\tag{41}
$$

They are deduced from four momentum conservation [20, 21]. In the above equation $s$ refers to the cms energy squared.

The momentum orientation (polar angle $\theta$ and azimuthal angle $\phi$) of scattered particle is decided by the assumption that the momentum transfer squared, $t$, is distributed as [19, 27]

$$
\frac{d\sigma}{dt} \sim \exp Bt,
\tag{42}
$$

$$
\alpha = 3.65(\sqrt{s} - m_1 - m_2) \approx 3.65\sqrt{s},
\tag{43}
$$

$$
B = \frac{\alpha^6}{1 + \alpha^6} A \approx A,
\tag{44}
$$

$$
A = \min(10.3, (1.12 < p_T >)^{-2}),
\tag{45}
$$

where $< p_T >$ stands for the mean transverse momentum assumed to be 0.5 GeV/c because it is observed in the experiment that the value of $< p_T >$ may be not so sensitive to the reaction energy and centrality [28]. In the above equations the second form was obtained provided the particle mass is negligible for high cms energy. On the other hand, $t$ is related to $\theta_s$ spanned between $\vec{p}_1$ and $\vec{p}_3$ [21] by

$$
t = m_1^2 - 2\epsilon_1\epsilon_3 + 2\vec{p}_1 \cdot \vec{p}_3 + m_3^2,
\tag{46}
$$

$$
t_{max} = m_1^2 - 2\epsilon_1\epsilon_3 + 2|\vec{p}_1||\vec{p}_3| + m_3^2,
\tag{47}
$$

$$
t_{min} = m_1^2 - 2\epsilon_1\epsilon_3 - 2|\vec{p}_1||\vec{p}_3| + m_3^2,
\tag{48}
$$

where $t_{max}$ and $t_{min}$ are corresponding to $\cos\theta_s = 1$ and -1, respectively. Therefore we first sample a $t'$ value within $[t_{min}, t_{max}]$ according to exponential distribution Eq. (42)

$$
t' = \frac{1}{B} \ln[\xi \exp(Bt_{max}) + (1 - \xi)\exp(Bt_{min})].
\tag{49}
$$

The corresponding $\cos\theta_s$ is then calculated by Eq. (46)

$$
\cos\theta_s = \frac{0.5(t' - m_1^2 - m_3^2) + \epsilon_1\epsilon_3}{|\vec{p}_1||\vec{p}_3|}.
\tag{50}
$$

The azimuthal angle $\phi_s$ is sampled isotropically in $2\pi$.

It should be mentioned that the orientation of scattered particle 3, for instance, is relative to scattering particle 1, so it should rotate back to the particle 1 and 2 cms system, where particle 1 is described by $|\vec{p}_1|$, $\theta_1$, and $\phi_1$. This rotation reads

$$
\begin{aligned}
p'_{3x} &= p_{3x}[\cos\phi_1(\cos\theta_1\sin\theta_s\cos\phi_s + \sin\theta_1\cos\theta_s) - \sin\phi_1\sin\theta_s\sin\phi_s], \\
p'_{3y} &= p_{3y}[\sin\phi_1(\cos\theta_1\sin\theta_s\cos\phi_s + \sin\theta_1\cos\theta_s) + \cos\phi_1\sin\theta_s\sin\phi_s], \\
p'_{3z} &= p_{3z}[\cos\theta_1\cos\theta_s - \sin\theta_1\sin\theta_s\cos\phi_s].
\end{aligned}
\tag{51}
$$

At last the scattered particles are boosted back to the moving frame of nucleus-nucleus cms system.

It is impossible to take all inelastic channels into account, only following inelastic reactions

$$
\begin{aligned}
\pi N &\rightleftharpoons \pi\Delta & \pi N &\rightleftharpoons \rho N, \\
N N &\rightleftharpoons N\Delta & \pi\pi &\rightleftharpoons k\bar{k}, \\
\pi N &\rightleftharpoons kY & \pi\bar{N} &\rightleftharpoons \bar{k}\bar{Y}, \\
\pi Y &\rightleftharpoons k\Xi & \pi\bar{Y} &\rightleftharpoons \bar{k}\bar{\Xi}, \\
\bar{k}N &\rightleftharpoons \pi Y & k\bar{N} &\rightleftharpoons \pi\bar{Y}, \\
\bar{k}Y &\rightleftharpoons \pi\Xi & k\bar{Y} &\rightleftharpoons \pi\bar{\Xi}, \\
\bar{k}N &\rightleftharpoons k\Xi & k\bar{N} &\rightleftharpoons \bar{k}\bar{\Xi}, \\
\pi\Xi &\rightleftharpoons k\Omega^- & \pi\bar{\Xi} &\rightleftharpoons \bar{k}\bar{\Omega}^-, \\
k\bar{\Xi} &\rightleftharpoons \pi\bar{\Omega}^- & \bar{k}\Xi &\rightleftharpoons \pi\Omega^-, \\
\end{aligned}
$$
$$N\bar{N}\,annihilation, N\bar{Y}\,annihilation,$$

are considered. The rest is treated as elastic reactions in a sense. Even so, there are already $\sim 600$ inelastic channels involved.

Taking $\pi N$ (re)scattering as an example, there are channels of

$$\pi N \rightarrow \pi\Delta, \quad \pi N \rightarrow \rho N, \quad \pi N \rightarrow kY, \tag{52}$$

therefore the relative probabilities of these channels are invoked to select one among them. The cross section of the reverse reactions are calculated by means of detailed balance.

The final state of $N\bar{N}$ and $N\bar{Y}$ annihilations are simply treated as five particle state through $N\bar{N} \rightarrow \rho\omega \rightarrow 5\pi$ and $N\bar{Y} \rightarrow k^*\omega \rightarrow k + 4\pi$, respectively. The cross section of $N\bar{Y}$ annihilation is assumed to be $1/5$ of the $N\bar{N}$ annihilation.

For elastic hadron (re)scattering because

$$m_1 = m_3, \quad m_2 = m_4, \quad |\vec{p}_1| = |\vec{p}_2| = |\vec{p}_3| = |\vec{p}_4|, \quad \epsilon_1 = \epsilon_3, \quad \epsilon_2 = \epsilon_4, \tag{53}$$

Eqs. (46)-(50) reduce, respectively, to

$$t = 2|\vec{p}_1|^2(\cos\theta_s - 1), \tag{54}$$
$$t_{max} = 0, \tag{55}$$
$$t_{min} = -4|\vec{p}_1|^2, \tag{56}$$

$$t' = \frac{1}{B}\ln[\xi + (1 - \xi)\exp(Bt_{min})], \tag{57}$$

$$\cos\theta_s = 1 + \frac{t'}{2|\vec{p}_1|^2}. \tag{58}$$

The rest is the same as that of inelastic (re)scattering.

### 2. Parton-parton collisions

If several partonic final states can be reached by a single partonic initial state the following relative probability is invoked to select one among them

$$\hat{\sigma}(ab \rightarrow cd; \hat{s})/\hat{\sigma}_{ab}(\hat{s}) \tag{59}$$

where

$$\hat{\sigma}(ab \rightarrow cd; \hat{s}) = \int_{-\hat{s}}^{0} \frac{d\hat{\sigma}}{d\hat{t}}(ab \rightarrow cd; \hat{s}, \hat{t})d\hat{t} \tag{60}$$

$$\hat{\sigma}_{ab}(\hat{s}) = \sum_{c,d} \hat{\sigma}(ab \rightarrow cd; \hat{s}). \tag{61}$$

In the inelastic parton-parton (re)scattering the flavor of scattered quark (antiquark) is decided according to

$$u : d : s : c \cdots = \gamma_u : \gamma_d : \gamma_s : \gamma_c \cdots \tag{62}$$

where $\gamma_u, \gamma_d, \gamma_s, \gamma_c, \cdots$ are input parameters and their default values are $1{:}1{:}0.3{:}10^{-11}\cdots$. The $c$ quark is not included presently.

The momentum transfer squared $\hat{t}$ is sampled according to

$$\Phi(\hat{t}) = \frac{1}{\hat{\sigma}(ab \to cd; \hat{s})} \int_{-\hat{s}}^{\hat{t}} \frac{d\hat{\sigma}}{d\hat{t}'}(ab \to cd; \hat{s}, \hat{t}')d\hat{t}'. \tag{63}$$

Then the (re)scattering angle is calculated by [20, 21]

$$\cos\theta_s = 1 + \frac{2\hat{s}\hat{t}}{[\hat{s} - (m_a + m_b)][\hat{s} - (m_a - m_b)]} \approx 1 + \frac{2\hat{t}}{\hat{s}} = 1 + \frac{\hat{t}}{2|\vec{p}_a|^2}, \tag{64}$$

where the second form is obtained provided the parton mass is negligible relative to the cms energy. The azimuthal angle is sampled randomly in $2\pi$.

## E.  Diquark break-up

In order to obtain the initial partonic state for nuclear collision system one has to switch-off string fragmentation in PYTHIA, to break-up the strings, and to break-up the diquarks in the strings. The diquark break-up is performed in its rest frame according to two-body decay kinematics [20, 21]. The energy and momentum modulus of broken quarks are calculated by Eq. (41) with $m_3$ and $m_4$ identified as the mass of broken quarks and $s$ the squared four momentum of diquark. The orientation of one of the broken quarks is sampled isotropically in $4\pi$ and the other is just orientated oppositely.

In the above, the three momentum of broken quark is calculated relative to three momentum of diquark, so it must be rotated back to the frame where diquark is described according to Eq. (51). It is also need to boost back to the moving frame of diquark according to inverse Lorentz transformation Eq. (21).

One of the broken quarks is assumed to have the diquark four position. The other is assumed to be created at the same time but is arranged randomly around the first one within 0.5 fm in each of the three position coordinates.

The gluons are also needed to be broken-up in the hadronization by the Monte Carlo coalescence model. Because of zero mass the gluon is broken according to three momentum conservation. The energy discrepancy between the breaking gluon and the broken quarks is shared among quarks and antiquarks. The flavor of broken quark is decided by Eq. (62).

## F.  Reduction of the strange (heavy) quark suppression

In the LUND string fragmentation regime the $q\bar{q}$ pair with quark mass $m$ and transverse momentum $p_T$ may be created quantum mechanically at one point and then tunnel out to the classically allowed region [15]. This tunnelling probability is given by

$$\exp(-\frac{\pi m^2}{\kappa})\exp(-\frac{\pi p_T^2}{\kappa}) \tag{65}$$

where the string tension $\kappa$ is assumed to be $\approx 1$ GeV/fm $\approx 0.2$ GeV$^2$ [15]. This probability implies a suppression of strange (heavy) quark production of $u : d : s : c \approx 1 : 1 : 0.3 : 10^{-11}$. The charm and heavier quarks are not expected to be produced in the soft string fragmentation process if there is no charm and heavier quarks in the string originally. They are expected to be produced only in the hard process or as a part of the initial- and final-state QCD radiations. The higher $p_T$ quark pair is expected to be created provided the string tension is large. However, in the PYTHIA 6.4 model there are model parameters of

- parj(1) is the suppression of diquark-antidiquark pair production compared with quark-antiquark production,

- parj(2) is the suppression of $s$ quark pair production compared with $u$ or $d$ pair production,

- parj(3) is the extra suppression of strange diquark production compared with the normal suppression of strange quark,

- parj(21) corresponds to the width $\sigma$ in the Gaussian $p_x$ and $p_y$ transverse momentum distributions for primary hadrons.

They are able to be tuned to reduce the strange quark suppression and to change the width of its $p_T$ distribution.

We introduced a mechanism of the increase of effective string tension and hence the reduction of strange quark suppression in [29]. In that paper we assumed that the effective string tension increases with the increasing of the number and hardening of gluons in the string by

$$\kappa^{eff} = \kappa_0 (1 - \xi)^{-a}, \tag{66}$$

$$\xi = \frac{\ln(\frac{k_{Tmax}^2}{s_0})}{\ln(\frac{s}{s_0}) + \sum_{j=2}^{n-1} \ln(\frac{k_{Tj}^2}{s_0})}. \tag{67}$$

In above equations, $\kappa_0$ is the string tension of the pure $q\bar{q}$ string assumed to be $\sim 1$ GeV/fm. The gluons in the multigluon string are ordered from 2 to n-1 because 1 and n refer to quark and antiquark at two ends of string. $k_{Tj}$ is the transverse momentum of gluon $j$ with $k_{Tj}^2 \geq s_0$ and $k_{Tmax}$ is the largest transverse momentum among the gluons. The parameters $a$=3.5 GeV and $s_0$=0.8 GeV were determined by fitting the hh collision data. It should be mentioned that Eq. (67) represents the deviation scale of the multigluon string from the pure string.

If $\lambda$ denotes parj(2) (parj(1), parj(3)) then by Eq. (65) the following relations between two strings with, respectively, effective string tension of $\kappa_1^{eff}$ and $\kappa_2^{eff}$ are obtained

$$\lambda_2 = \lambda_1^{\frac{\kappa_1^{eff}}{\kappa_2^{eff}}}, \tag{68}$$

$$\sigma_2 = \sigma_1 (\frac{\kappa_2^{eff}}{\kappa_1^{eff}})^{1/2}, \tag{69}$$

where subscripts identify the strings.

Above mechanism is involved in the PACIAE 2.0 model. Therefore one can first tune the parameters of parj(1), (2), (3), and (21) to fit the strangeness production data in a given nuclear collision at a given energy. Then the resulted parj(1), (2), (3), (21) and effective string tension can be used to predict the strangeness production in the same reaction system at different energy even in the different reaction systems.

## G. Deexcitation of the energetic quark (antiquark) in coalescence model

If the energy of a quark (anti-quark) is large enough (e.g. >2 GeV), one should introduce deexcitation mechanism for this quark (antiquark) in the coalescence model. This is similar to the iterative approach of quark-antiquark pair generation in the LUND string fragmentation regime [13, 15, 16]. Taking an energetic initial quark $q_0$ as an example, a new $q_1\bar{q}_1$ pair may be created from vacuum. This quark-antiquark pair brings a fraction $z$ of energy (momentum) of $q_0$ and leaves remnant of $q_0$ behind. If the energy of $q_0$ remnant is still large enough, a new $q_2\bar{q}_2$ pair creates and above processes repeats until the energy is not enough to generate a new quark-antiquark pair.

In the case of positive longitudinal momentum of mother quark $p_{0z}$ in order to obtain four momentum of the first daughter pair $q_1\bar{q}_1$ we introduce the forward light cone variable

$$W_0 = E_0 + p_{0z}. \tag{70}$$

The LUND string fragmentation function

$$f(z) \propto z^{-1}(1 - z)^\alpha \exp(-\beta m_T^2/z) \tag{71}$$

with default values of $\alpha = 0.3$ and $\beta = 0.58$ or the Field-Feynman parametrization

$$f(z) \propto 1 - \alpha + 3\alpha(1-z)^2 \qquad (72)$$

with default value of $\alpha = 0.77$ is used to sample randomly a fraction variable $z_1$ for the first daughter pair $q_1\bar{q}_1$. Its forward light cone variable is then

$$W_1 = z_1 W_0. \qquad (73)$$

From Eqs. (70) and (73), we obtain

$$E_1 = \frac{1}{2}(W_1 + \frac{m_{1T}^2}{W_1}), \qquad (74)$$

$$p_{1z} = \frac{1}{2}(W_1 - \frac{m_{1T}^2}{W_1}). \qquad (75)$$

Similarly, for the negative longitudinal momentum of mother quark, one has to introduce the backward light cone variable

$$w_0 = E_0 - p_{0z} \qquad (76)$$

and has the solution of

$$E_1 = \frac{1}{2}(W_1 + \frac{m_{1T}^2}{W_1}), \qquad (77)$$

$$p_{1z} = -\frac{1}{2}(W_1 - \frac{m_{1T}^2}{W_1}), \qquad (78)$$

for the first daughter pair $q_1\bar{q}_1$.

The $p_{1x}$ and $p_{1y}$ of $q_1\bar{q}_1$ pair are sampled according to the two dimensional Gaussian distribution [30]

$$\exp[-p_T^2/\sigma]dp_T^2, \qquad\qquad 0 < p_T^2 < p_{Tmax}, \qquad (79)$$

with default values of $\sigma$=0.5 $(\text{GeV/c})^{-2}$, $p_{Tmax}$=6 GeV/c. Then we obtain

$$p_{1x} = p_{1T}\cos(\phi), \qquad\qquad p_{1y} = p_{1T}\sin(\phi), \qquad (80)$$

with $\phi$ sampled isotropically in $2\pi$.

The $q_1\bar{q}_1$ pair is then broken up in its rest frame according to two-body kinematics mentioned above. The flavor of quark (antiquark) is sampled according to Eq. (62). It is also needed first to rotate back to the frame where $q_1\bar{q}_1$ pair is described according to Eq. (51) and then to boost back to the moving frame of $q_1\bar{q}_1$ pair according to inverse Lorentz transformation Eq. (21).

## III.  PROGRAM (MODEL) STRUCTURE

PACIAE 2.0 has three versions: PACIAE 2.0a (its program packets are compressed to 20a.tar.gz) describing the relativistic elementary collisions (pp, $\bar{\text{p}}$p, or $e^+e^-$) and PACIAE 2.0b (20b.tar.gz) as well as PACIAE 2.0c (20c.tar.gz) describing the relativistic nucleus-nucleus (A+B, including p+A) collisions.

### A.  PACIAE 2.0a structure

The PACIAE 2.0a model is for elementary collisions, it differs from PYTHIA 6.4 in the addition of the parton rescattering before hadronization and the hadron rescattering after hadronization. In order to create the initial partonic state we switch off the string fragmentation temporarily in the PACIAE 2.0 model. Then we obtain a partonic initial state (parton list) after the strings are broken up and the diquarks (anti-diquarks) are split up randomly. This partonic matter proceeds parton rescattering. After parton rescattering the partonic matter is hadronized by the string fragmentation or Monte Carlo coalescence model. The hadronic rescattering is followed. Therefore the PACIAE 2.0a, as well as PA-CIAE 2.0b and PACIAE 2.0c, consists of the parton initiation, parton evolution (cascade, rescattering), hadronization, and hadron evolution (cascade, rescattering) four stages.

PACIAE 2.0a program consists of paciae_20a.f, parcas_20a.f, sfm_20a.f, coales_20a.f, hadcas_20a.f, and p_20a.f:

1. paciae_20a.f plays both functions of an example of user program and parton initiation. The later is performed by PYTHIA with the string fragmentation switched-off and the diquarks broken-up randomly. We obtain a configuration of quarks, anti-quarks, gluons, and a few hadronic remnants. This is a partonic initial state (parton list) for an elementary collision.

2. parcas_20a.f performs the parton rescattering based on the parton list above. The key ingredients of this cascade process were:

   - The partons are assumed traveling on the straight trajectories along their momentum direction.
   - The partons interact with each other by the $2 \to 2$ LO pQCD cross section $\sigma_{tot}$ [24, 25] or its variety of keeping only leading divergent terms. With the collision times of all possible interaction pairs the collision time list is composed.
   - A parton-parton collision pair with least collision time is selected from the collision time list and executed according to the LO pQCD differential and total cross sections.
   - Update the parton list by removing the scattering partons and adding the scattered (generated) partons.
   - Update the collision time list by removing the collision pairs containing any one of the scattering partons and adding the new collision pairs constructed by one of the scattered (generated) partons with another one in parton list.
   - A new parton-parton collision pair with least collision time is selected from the collision time list.
   - Repeat last four items until the collision time list is empty (partonic freeze-out).

3. sfm_20a.f executes the hadronization of partonic matter according to the LUND string fragmentation after the parton rescattering and string reconstruction by calling p20a.f.

4. coales_20a.f performs the hadronization of partonic matter according to the Monte Carlo coalescence model after the parton rescattering. The key ingredients of this coalescence model are:

   - The energetic partons are first deexcited.
   - The gluons are forcibly split into $q\bar{q}$ pair randomly.
   - A hadron table, composed of mesons and baryons, inputted to the program. The pseudoscalar and vector mesons made of u, d, s, and c quarks, the $B^+$, $B^0$, $B^{*0}$, as well as $\Upsilon$ are considered as mesons. The baryons include the SU(4) multiplets of baryons made of u, d, s, and c quarks (except those with double c quarks) and $\Lambda_b^0$.
   - Two partons coalesce a meson and three partons a baryon (antibaryon) in hadron table according to the quark flavor structure of the coalesced hadron and the flavors, positions, as well as momenta of the coalescing partons.
   - If the coalescing partons can form either a pseudoscalar meson or a vector meson (e. g. $u\bar{d}$ can be a $\pi^+$ or a $\rho^+$) the principle of less discrepancy between the invariant mass of coalescing partons and the mass of coalesced hadron is invoked to select one from them. The same principle is used in the baryon production (such as $p$ and $\Delta^+$ are composed of $uud$).
   - The momentum conservation is required.
   - The phase space constraint

   $$\frac{16\pi^2}{9}\Delta r^3 \Delta p^3 = \frac{h^3}{d} \tag{81}$$

   is introduced as an option. In the above equation $h^3/d$ is the volume occupied by a single hadron in the phase space, $d=4$ refers to the spin and parity degeneracies of hadron, $\Delta r$ and $\Delta p$ stand for the position and momentum distances between coalescing partons, respectively.

   One selects sfm_20a.f or coales_20a.f to hadronize the partonic matter by switch parameter adj1(12).

5. hadcas_20a.f executes hadron rescattering after hadronization. This hadron cascade proceeds in the same way as the one in the parton cascade mentioned above. But one should note:

   - The hadrons of $\pi, k, p, n, \rho(\omega), \Delta, \Lambda, \Sigma, \Xi, \Omega, J/\Psi$ and their antiparticles are considered here instead of parton there.
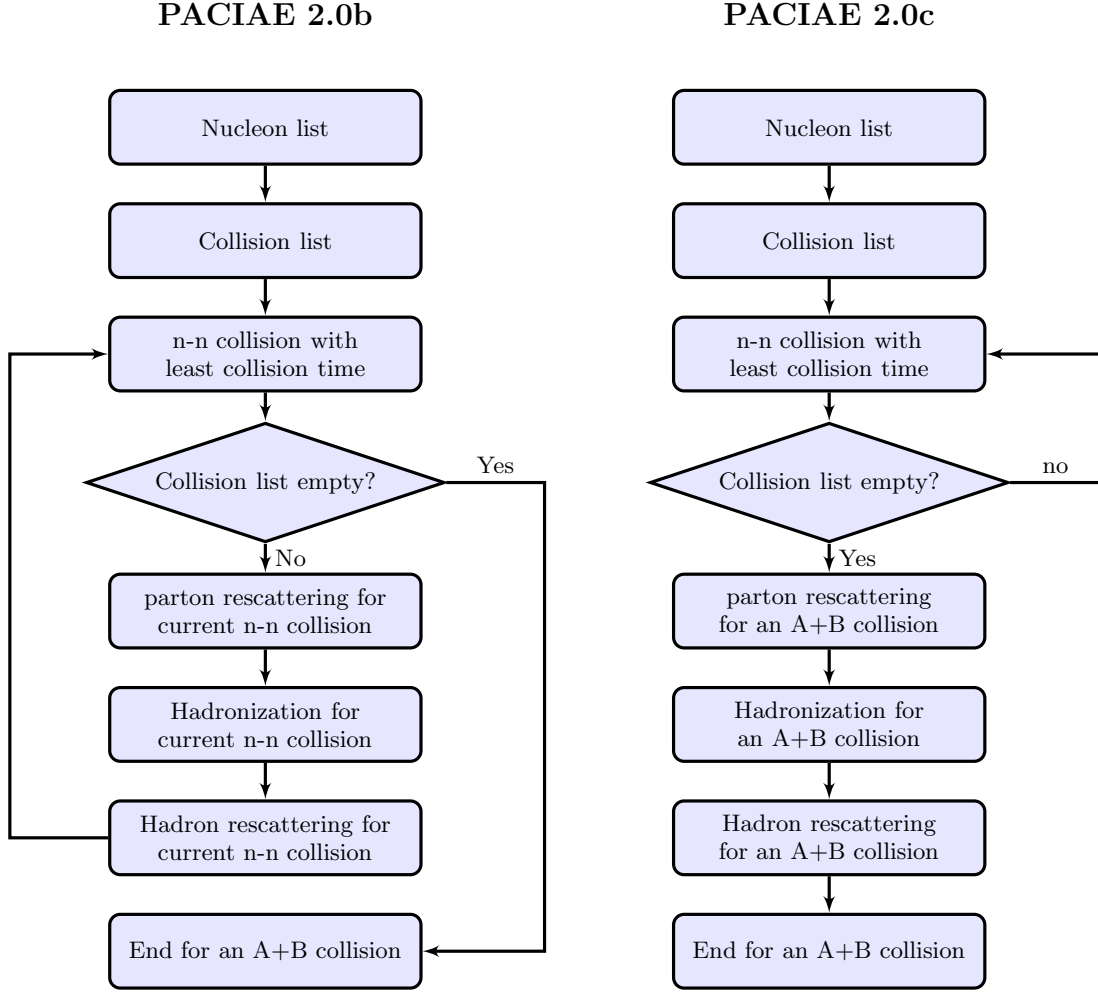
FIG. 1: Structure of PACIAE 2.0b (left) and PACIAE 2.0c (right) for the dynamical simulation of a nucleus-nucleus (A+B) collision.

- Instead of LO pQCD parton-parton cross section is the hh total cross section.

6. p20a.f is different from PYTHIA 6.4 in the addition of mechanism for the reduction of strange quark suppression.

7. usux.dat is an example for input file. Each program packet (paciae_20a.f, parcas_20a.f, ...) is flexibly to be modified and/or replaced. A run can stop at the end of any packet for different purposes. For instance, one just sets the switch parameter adj1(40)=1 if one takes interest in the partonic output before parton rescattering.

TABLE I: Charged particle pseudorapidity densities at mid-rapidity ($|\eta| < 1$) for the INEL pp collisions having at least one charged particle in the same region (INEL$> 0_{|\eta|<1}$) at $\sqrt{s}$=0.9, 2.36, and 7 TeV measured by ALICE [32]. The first data error is statistical and the second systematic. The corresponding results calculated by PYTHIA 6.4 and PACIAE 2.0a were given as well.

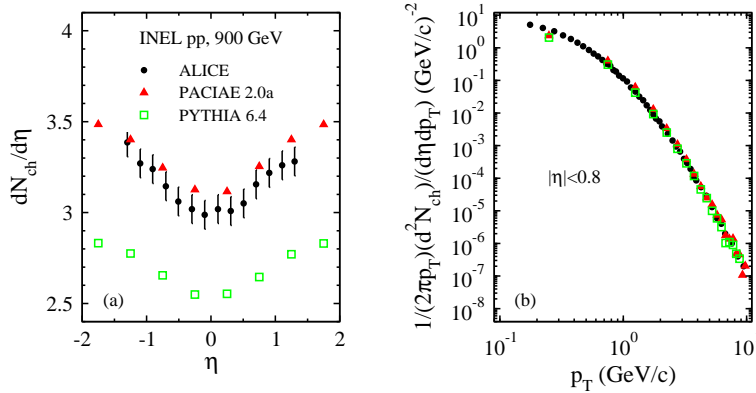| $\sqrt{s}$ TeV | ALICE | PYTHIA | PACIAE 2.0a |
|---|---|---|---|
| 0.9 | 3.81±0.01±0.07 | 3.35 | 3.62 |
| 2.36 | 4.70±0.01±0.10 | 4.07 | 4.45 |
| 7 | 6.01±0.01±0.16 | 5.25 | 5.95 |

FIG. 2: (Color online) (a) charged particle pseudorapidity distribution in INEL pp collisions at $\sqrt{s}$=900 GeV measured by ALICE [33] and compared with the PACIAE 2.0a and PYTHIA 6.4 results. (b) transverse momentum distribution where data taken from [34].

## B.   PACIAE 2.0b structure

PACIAE 2.0b program consists of paciae_20b.f, parini_20b.f, parcas_20b.f, sfm_20b.f, colaes_20b.f, hadcas_20b.f, and p20b.f:

1. paciae_20b.f is a user program.

2. parini_20b.f administrates the generation of an event for an A+B collision:

   - Initiation in the position and momentum spaces for an A+B collision:
     - One colliding nucleus is set on the origin in the position space and the other on the position apart from the origin by an impact parameter $b$ in the $x$ axis. Both nucleus centers are assumed having $y = z = 0$. The colliding nucleus is assumed geometrically as a sphere with radius $R_{A(B)}$ fm.
     - The geometric number of participant nucleons is first calculated. Then the participant nucleons are arranged randomly in the overlap region of the colliding nuclei. The rest nucleons in the colliding nucleus are randomly arranged in the corresponding sphere according to the Woods-Saxon distribution (for radius $r$) and $4\pi$ isotropic distribution (for orientation) and are required to be outside the overlap region.
     - The beam momentum is given to the nucleons in the colliding nucleus properly.
     - An initial nucleon list for an A+B collision is then obtained.

TABLE II: Total charged multiplicity in 0-6% most central Au+Au collisions at $\sqrt{s_{NN}}$=0.2 GeV [2] and the charged particle pseudorapidity density at mid-rapidity ($|\eta|$ <0.5) in 0-5% most central Pb+Pb collisions at $\sqrt{s_{NN}}$=2.76 TeV [33] as well as the corresponding results calculated by PACIAE 2.0b, 2.0c, and 2.0c_c (the same as PACIAE 2.0c but hadronized by the Monte Carlo coalescence instead of the string fragmentation).

| Reaction | $\sqrt{s_{NN}}$ TeV | Exp. | PACIAE 2.0b | PACIAE 2.0c | PACIAE 2.0c_c |
|---|---|---|---|---|---|
| Au+Au | 0.2 | 5060±250[†] | 4940 | 4961 | 4746 |
| Pb+Pb | 2.76 | 1601±60[‡] | 1554 | 1542 | 1540 |

[†] taken from [2].   [‡] taken from [35].

- The nucleons in one colliding nucleus interact with nucleons in the other one when they traveling along their straight trajectories according to the NN total cross section. The corresponding collision time is calculated for all possible collision pairs and then the initial NN (hh) collision time list is composed.

- A NN collision pair with least collision time is selected from the NN (hh) collision time list. This NN (hh) collision, if its cms energy is large enough ($\sqrt{s} \geq$4.5 GeV, for instance), executes by PYTHIA with the string fragmentation switched-off and diquarks broken-up. A parton
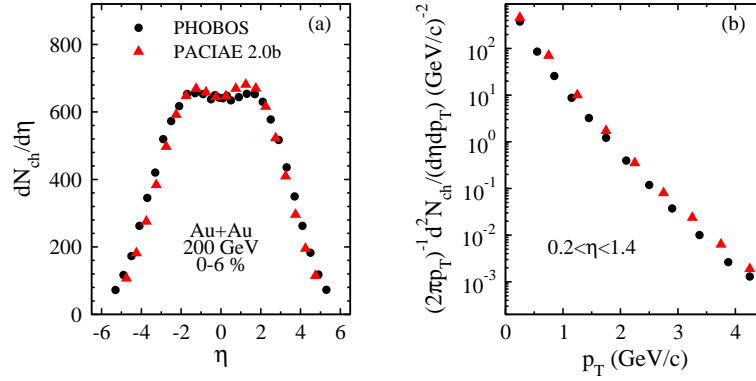
FIG. 3: (Color online) (a) charged particle pseudorapidity distribution in 0-6% most central Au+Au collisions at $\sqrt{s_{NN}}$=200 GeV measured by PHOBOS [2] and compared with the PACIAE 2.0b results. (b) transverse momentum distribution where data taken from [36]).

    configuration (parton list) for this NN (hh) collision is then obtained. If the energy is not large enough the NN (hh) collision is dealt with the usual two-body elastic collision [19].

- A parton cascade, the same as the one mentioned in last subsection, proceeds for current NN (hh) collision by parcas_20b.f.

- sfm_20b.f or coales_20b.f executes the hadronization of partonic matter in current NN (hh) collision by the LUND string fragmentation regime (calling p20b.f) or Monte Carlo coalescence model according to the switch parameter adj1(12). sfm_20b.f and coales_20b.f are some what different from sfm_20a.f and coales_20a.f in PACIAE 2.0a, respectively. p20b.f is different from PYTHIA 6.4 in the addition of the mechanism for the reduction of strange quark suppression and of the treatment for the charge conservation in fragmentation of a string.

- hadcas_20b.f performs hadron rescattering after hadronization of current NN (hh) collision. It is similar to the hadron rescattering in PACIAE 2.0a.

- Update the nucleon (hadron) list and NN (hh) collision time list after current NN (hh) collision executed.

- A new NN (hh) collision pair with least collision time is selected from the NN (hh) collision time list.

- Repeat above six items until the NN (hh) collision time list is empty (hadronic freeze-out).

3. A hadronic final state is eventually obtained for an A+B collision after the execution of parini_20b.f.

4. usu.dat is an example for input file. The left panel of Fig. 1 shows the structure of PACIAE 2.0b program for the dynamical simulation of a nucleus-nucleus collision.

### C.   PACIAE 2.0c structure

    PACIAE 2.0c program consists of paciae_20c.f, parini_20c.f, parcas_20c.f, sfm_20c.f, colaes_20c.f, hadcas_20c.f44, and p20c.f:

1. paciae_20c.f plays double roles of the user program (an example) and the administrating an A+B collision event generation.

2. parini_20c.f performs the parton initiation for an A+B collision. It is indeed a nucleon cascade process:

- Initiation in the position and momentum spaces for an A+B collision is the same as that in PACIAE 2.0b.

- The initial NN collision time list is also constructed as the same as that in PACIAE 2.0b.

- A NN collision pair with least collision time is selected from the NN collision time list.
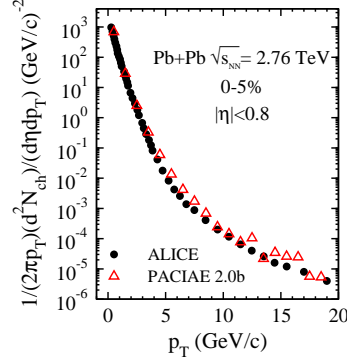
FIG. 4: (Color online) Charged particle transverse momentum distribution in 0-5% most central Pb+Pb collisions at $\sqrt{s_{NN}}$=2.76 TeV measured by ALICE [37] and compared with the PACIAE 2.0b results.

- This NN collision, if energy is large enough, executes by PYTHIA with the string fragmentation switched-off and the diquarks broken-up. The generated partons are filled in the parton list. If the energy is not large enough the current NN collision is dealt with usual two-body elastic collision [19].

- Update the nucleon list and NN collision time list.

- A new NN collision pair with least collision time is selected from the NN collision time list.

- Repeat above three items until the NN collision time list is empty (hadronic freeze-out). Then one obtains a partonic initial state (parton list) for an A+B collision.

3. parcas_20c.f performs the parton rescattering for an A+B collision.

4. sfm_20c.f executes the hadronization by the LUND string fragmentation regime (by calling p20c.f) for an A+B collision if switch parameter adj1(12)=0.

5. coales_20c.f performs the hadronization for an A+B collision by the Monte Carlo coalescence model if switch parameter adj1(12)=1.

6. hadcas_20c.f executes the hadron rescattering for an A+B collision.

7. p20c.f is different from PYTHIA 6.4 in the addition of the mechanism for reduction of the strange quark suppression and of the requirement for charge conservation in the fragmentation of a string.

The right panel of Fig. 1 shows the structure of PACIAE 2.0c program for the dynamical simulation of a nucleus-nucleus collision. Comparing left panel with right panel in Fig. 1, one knows that in the PACIAE 2.0b model the parton initiation, parton rescattering, hadronization, and hadron rescattering are performed for each hh collision pair independently. This is similar to the Monte Carlo Glauber model [31] despite that it is only a hadronic cascade model. PACIAE 2.0b characterizes the correlations among above processes for each hh collision pair, but there are no correlations among different hh collision pairs. This also means that in PACIAE 2.0b the nucleus-nucleus collision is dealt as a superposition of the nucleon-nucleon collisions in a sense. Hence the PACIAE 2.0b model presents the locality. Oppositely, the PACIAE 2.0c model characterizes the correlations among the different hh collision pairs in each process of the parton initiation, parton rescattering, hadronization, and hadron rescattering, but there are no correlations among above processes for each hh collision pair. PACIAE 2.0b and 2.0c are similar in the physical contents but are different in the topological structure.

In order to decrease the line number in common block 'pyjets', a special common block 'sgam' is introduced. The photon is removed from 'pyjets' to 'sgam' after generation and is given specific flavor code as follows:

- 22: hardonic decay photon,

- 44: prompt direct photon,

- 55: photon from parton-parton rescattering

$$q + g \rightarrow q + \gamma, \qquad\qquad q + \bar{q} \rightarrow g + \gamma, \qquad\qquad (82)$$
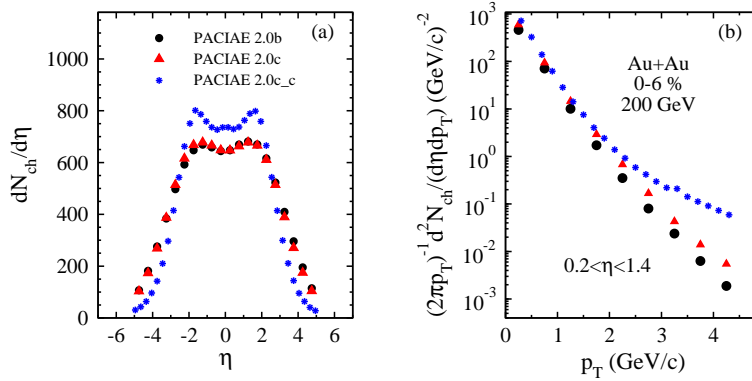
FIG. 5: (Color online) (a) charged particle pseudorapidity distribution in Au+Au collisions at $\sqrt{s_{NN}}$=200 GeV calculated by the PACIAE 2.0b (circles), PACIAE 2.0c (triangles), and PACIAE 2.0c_c (stars). (b) transverse momentum distribution.

- 66: hardonic direct photon

$$\pi + \pi \rightarrow \rho + \gamma, \qquad\qquad \pi + \rho \rightarrow \pi + \gamma. \qquad\qquad (83)$$

In default versions of PACIAE 2.0, the inelastic processes, $q\bar{q} \rightarrow gg$ (denoted as process 6 in the program) and $gg \rightarrow q\bar{q}$ (process 7), are switched-off. If one wishes to include the inelastic process one has to comment out the statement of 'fsqq=0' and/or 'fsgg_1=0' in parcas_20a.f (or parcas_20b.f, or parcas_20c.f).

## IV.   EXAMPLES CALCULATED

The model parameters in PYTHIA 6.4 and PACIAE 2.0 were given default values according to the experimental measurement and/or the physical argument. However, in the specific calculations, a few sensitive parameters, as least as possible, should be tuned to a datum of the global measurable, such as the charged multiplicity or the charged particle rapidity density at mid-rapidity. The fitted parameters were then used to investigate the other physical observables.

In the PACIAE 2.0a calculations the K factor was tuned to the charged particle pseudorapidity density at mid-pseudorapidity ($|\eta| < 1$) in the INEL (inelastic) pp collisions having at least one charged particle in the same region (INEL$> 0_{|\eta|<1}$) at $\sqrt{s}$=0.9, 2.36, and 7 TeV [32]. The results were shown in Tab. I together with the ALICE data [32]. This fitted K=1.9 (D=1.5, D means default value) was employed to calculate the charged particle pseudorapidity distribution and transverse momentum distribution ($|\eta| < 0.8$) in the INEL pp collisions at $\sqrt{s}$=0.9 TeV. These results were compared with the ALICE data [33, 34] in Fig 2. One sees in this figure that the ALICE data are reproduced reasonably.

We have used PACIAE 2.0b to calculate the 0-6% most central Au+Au collisions at $\sqrt{s_{NN}}$=200 GeV and 0-5% most central Pb+Pb collisions at $\sqrt{s_{NN}}$ =2.76 TeV. In these calculations the K factor, the parameter $\beta$ in LUND string fragmentation function, and the time accuracy $\Delta t$ (the least time interval of two distinguishably consecutive collisions in the parton initiation stage) were tuned to the PHOBOS data of charged multiplicity [2] and the ALICE data of charged particle pseudorapidity density at mid-rapidity ($|\eta| < 0.5$) [35], respectively. The results were given in Tab. II. The fitted parameters of K=1.7 (D=1.5), $\beta$=1.5 (D=0.58), and $\Delta t$=0.0001 for Au+Au as well as K=1.7, $\beta$=1.5, and $\Delta t$ =0.00004 for Pb+Pb were then employed to calculate the charged particle pseudorapidity distribution and transverse momentum distribution in Au+Au collisions and the transverse momentum distribution in Pb+Pb collisions by PACIAE 2.0b, respectively. These results were compared with the PHOBOS [2, 36] and the ALICE [37] data in Fig. 3 and 4, respectively. We see in these figures that the experimental data are well described. The large fluctuation of the theoretical data at the tail of transverse momentum distribution in Fig. 4 is because the total events of 1000 calculated is not enough.

Similar calculations were also performed by PAICIA 2.0c and PAICIA 2.0c_c (which is the same as PACIAE 2.0c but hadronized by the Mote Carlo coalescence instead of the string fragmentation ). In the PAICIA 2.0c calculations K=1.7, $\beta$=0.58, and $\Delta t$=0.0001 were assumed for Au+Au collisions and K=1.7, $\beta$=0.58, and $\Delta t$=0.00001 for Pb+Pb collisions. The parameters of K=1.7 and $\Delta t$=0.0001 for

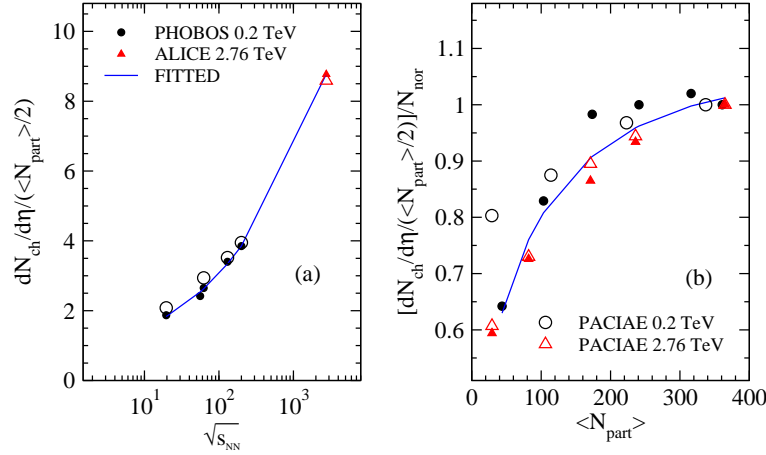FIG. 6: (Color online) (a) Energy dependence of the participant scaled charged particle pseudorapidity density $dN_{ch}/d\eta/(N_{part}/2)$ at midrapidity in 0-6% most central Au+Au collisions at RHIC energies and 0-5% Pb+Pb collisions at LHC energy. (b) Centrality dependence, where $N_{nor}$ indicates $dN_{ch}/d\eta/(N_{part}/2)$ at largest $N_{part}$. In this figure the curves are fitted results and the open symbols are results from PACIAE 2.0b calculations.

Au+Au collisions as well as K=1.7 and $\Delta t$=0.000055 for Pb+Pb collisions were assumed in PAICIA 2.0c_c calculations. The results of charged particle multiplicities were compared with the results from PACIAE 2.0b calculations and the experimental data in Tab. II. Fig. 5 gave the comparison of the charged particle pseudorapidity (panel (a)) and transverse momentum (panel (b)) distributions with the corresponding PACIAE 2.0b results above. We see in this figure that PAICIA 2.0c is also able to describe the experimental data. However, the discrepancy between PAICIA 2.0c and PAICIA 2.0c_c is visible.

Recently, PHOBOS investigated the energy dependence of the participant scaled charged particle pseudorapidity density at mid-rapidity $dN_{ch}/d\eta/(N_{part}/2)$ in the relativistic pp and A+B collisions. They obtained the function of $dN_{ch}/d\eta/(N_{part}/2)$ vs. $\sqrt{s_{NN}}$ by fitting the experimental data spanned from 10 GeV to 7 TeV for pp and from 2 GeV to 200 GeV for A+B collisions [1] (Before the submission of this paper we knew that PHOBOS just published their paper in Phys. Rev. C where they added a fitting of the experimental data from 19.6 GeV to 2.76 TeV with a power law in $\sqrt{s_{NN}}$ for A+B collisions.). Assuming further that the dependence of $dN_{ch}/d\eta/(N_{part}/2)$ on energy and centrality (denoted by Glauber model $N_{part}$) can be factorized, then they obtained the function of $dN_{ch}/d\eta/(N_{part}/2)$ vs. $\sqrt{s_{NN}}$ and the function of $dN_{ch}/d\eta/(N_{part}/2)$ vs. $N_{part}$.

We used the geometric number of participant nucleons instead of the Glauber model $N_{part}$ to fit first the PHOBOS data of 0-6% most central Au+Au collisions at RHIC energies [1] and ALICE datum of 0-5% most central Pb+Pb collisions at $\sqrt{s_{NN}}$=2.76 TeV [35] (cf. Fig. 6 (a)). Then we fitted the PHOBOS centrality dependence data [1] with normalization to the datum of highest centrality (i. e. $N_{nor}$ in the figure) and ALICE centrality dependence data [35] with similar normalization (cf. Fig. 6(b)). The fitted functions were obtained

$$z = f(x)\frac{g(y)}{g(y_{max})}, \tag{84}$$

$$f(x) = 0.2\ln(x) + 0.001788(\ln(x))^2 + 0.01244(\ln(x))^3 + 0.8916, \tag{85}$$

$$g(y) = -0.2217 + 0.3088y^{(1/3)} - 0.01906y^{(2/3)}, \tag{86}$$

where $z, x$, and $y$ denoted $dN_{ch}/d\eta/(N_{part}/2)$, $\sqrt{s_{NN}}$, and $N_{part}$, respectively.

We fitted the PHOBOS pp data [1] and ALICE pp data [32] of $dN_{ch}/d\eta$ by the function as the same as Eq. (85). The new four coefficients of 1.725, -0.1312, 0.007777, and -4.3842 were obtained (cf. Fig. 7).

With above fitted relations one may be able to first predict $dN_{ch}/d\eta/(N_{part}/2)$ for un-measured pp and/or A+B collisions in the RHIC and LHC energy region. Then tuning the sensitive model parameters (such as K factor, $\beta$, and/or $\Delta t$ above) to this $dN_{ch}/d\eta/(N_{part}/2)$ one may also be able to predict other observables such as pseudorapidity distribution, transverse momentum distribution, etc..
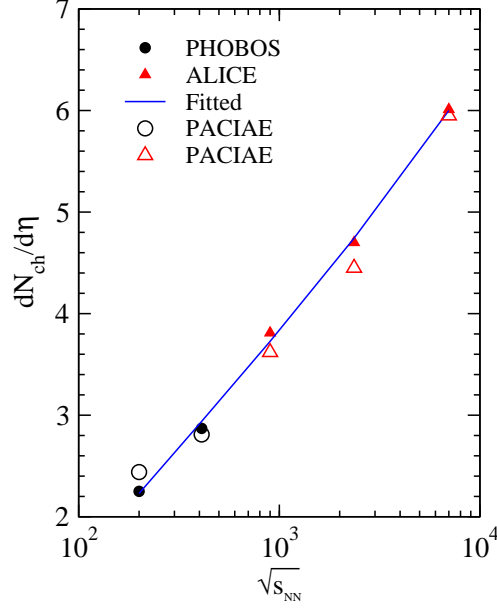
## ACKNOWLEDGEMENT

FIG. 7: (Color online) Energy dependence of the participant scaled charged particle pseudorapidity density $dN_{ch}/d\eta$ at midrapidity in pp collisions at RHIC and LHC energies. The curve is fitted results and the open symbols are results from PACIAE 2.0a calculations.

## APPENDIX: PACIAE 2.0 USERS' GUIDE

1. **Selection of the processes**
   A switch variable (nchan) is introduced as follows:

   - nchan=0: Inelastic (INEL),

   - nchan=1: Non Single Diffractive (NSD),

   - nchan=2: $q\bar{q} \to \gamma^*/Z^0$ used to generate Drell-Yan process,

   - nchan=3: J/$\psi$ production,

   - nchan=4: heavy-flavor production,

   - nchan=5: direct photon.

   - nchan=6: soft processes only,

   - nchan=7: default PYTHIA.

2. **Run PACIAE**

   - Compile each of the FORTRAN program packets in 20a.tar.gz or 20b.tar. gz or 20c.tar.gz and link them together forming an executable file.

   - Set the parameters in input file of usux.dat for PACIAE 2.0a or usu.dat for PACIAE 2.0b and PACIAE 2.0c properly.

   - Run the executable file.

3. **Parameters**
   The parameters introduced in PACIAE 2.0, except those in PYTHIA 6.4, can be found in the read statements in user program of paciae_20a.f (paciae_20b.f, paciae_20c.f). Meaning of parameter can be found in the program packets via searching its name. Those parameters not described in the program packets and the array adj1(40) are explained as follows:

- nout: internal output per 'nout' events.

- psno=1: systematic sampling method for impact parameter in A+B collisions,
  psno=2: randomly sampling method for impact parameter.
  To run an event with a given impact parameter, set 'bmin'='bmax' in usu.dat.

- adj1(i), i=

1: K factor in parton cascade.
2: $\alpha_s$, effective coupling constant in the parton rescattering (cascade).
3: parameter 'tcut' ($\hat{t}_{cut}$) introduced in the integration of parton-parton differential
   cross section in the subroutine 'fsig' in parcas_20a.f (parcas_20b.f, parcas_20c.f).
4: parameter 'idw', the number of intervals in the numerical integration
   in parcas_20a.f (parcas_20b.f, parcas_20c.f).
5: =1 with nuclear shadowing,
   =0 without nuclear shadowing.
6: parameter $\alpha$ (parj(41) in PYTHIA 6.4) in the LUND string fragmentation function.
7: parameter $\beta$ (parj(42) in PYTHIA 6.4) in the LUND string fragmentation function.
8: mstp(82) in PYTHIA 6.4
   =1, with hard interactions,
   =0: without hard interactions (simple two-string model, soft only).
9: parp(81) in PYTHIA 6.4 (default=1.4 GeV/c), effective minimum transverse momentum for
   multiple interactions when mstp(82)=1.
10: K factor (parp(31) in PYTHIA 6.4).
11: time accuracy used in the hadron cascade (hadcas_20a.f, hadcas_20b.f, and hadcas_20c.f).
12: model for hadronization
    =0 string fragmentation,
    =1 Monte Carlo coalescence model.
13: dimension of meson table considered.
14: dimension of baryon table considered.
15: string tension.
16: number of loops in the deexcitation of energetic quark in the Monte Carlo coalescence model.
17: the threshold energy in the deexcitation of energetic quark in the Monte Carlo coalescence model.
18: =0 without Pauli blocking in the parton cascade,
    =1 with Pauli blocking.
19: time accuracy used in the parton cascade (parcas_20a.f, parcas _20b.f, and parcas_20c.f).
20: =0 using LO pQCD parton-parton cross section in the parton rescattering (cascade),
    =1 using keeping only leading divergent terms in the LO pQCD parton-parton cross section,
    =2 the same as 0 but flat scattering angle distribution is assumed,
    =3 the same as 1 but flat scattering angle distribution is assumed.
21: =0 without phase space constraint in the Monte Carlo coalescence model,
    =1 with phase space constraint.
22: critical value of the product of radii in the position and momentum phase spaces (4 is assumed).
23: =0 LUND string fragmentation function is used in the subroutine for deexcitation of the
    energetic quark in the Monte Carlo coalescence model,
    =1 Field-Feynman parametrization function is used.
24: the virtuality cut ('tl0') in the time-like radiation in the parton rescattering (cascade).
25: $\Lambda_{QCD}$ in the parton cascade.
26: number of random number thrown away.
27: largest momentum allowed for particle.
28: concerned to the largest position allowed for particle, see program for the detail.
29: width of two dimension Gaussian distribution sampling $p_x$ and $p_y$ of the produced quark
    pair in the deexcitation of energetic quark in the Monte Carlo coalescence model.
30: maximum $p_T^2$ in above two dimension Gaussian distribution.
31: parj(1) in PYTHIA 6.4.
32: parj(2) in PYTHIA 6.4.
33: parj(3) in PYTHIA 6.4.
34: parj(21) in PYTHIA 6.4.
35: mstp(91) in PYTHIA 6.4, parton transverse momentum ($k_\perp$) distribution inside hadron;
    =1, Gaussian;

=2, exponential

36: =0 without phenomenological parton energy loss in the parton rescattering (cascade),
=1 with phenomenological parton energy loss.

37: the coefficient in phenomenological parton energy loss.

38: $p_T$ cut in phenomenological parton energy loss.

39: width of Gaussian $k_\perp$ distribution in hadron if mstp(91)=1,
width of exponential $k_\perp$ distribution in hadron if mstp(91)=2.

40: decide where the run stopped:
=1, after parton initiation;
=2, after parton rescattering;
=4, after hadron rescattering.

4. **Output files**

- rms0.out is an output for the input parameters.

- rms.out is the main output file.

- main.out is the PYTHIA standard output.

- oscar.out is the OSCAR standard output if nosc=2 or 3.

- Encourage user to write his/her own output file and user program.

5. **Postscript**

- The PACIAE 2.0 program is free for the person who is interested. However, it is protected by GPL, no merchandise use please.

- Welcome reporting any bugs to yanyl@ciae.ac.cn, zhoudm@phy.ccnu.edu.cn , and/or sabh@ciae.ac.cn .

# REFERENCES

[1] B. Alver, et al., PHOBOS Collab., arXiv:1011.1940v1, Phys. Rev. C **83**, 024913 (2011).
[2] B. B. Back, et al., PHOBOS Collab., Phys. Rev. Lett. **91**, 052303 (2003).
[3] C. Adler, et al., STAR Collab., Phys. Rev. Lett. **87**, 112303 (2001).
[4] K. Adcox, et al., PHENIX Collab., Phys. Rev. Lett. **88**, 022301 (2002).
[5] X.-N. Wang and M. Gyulassy, Phys. Rev. Lett. **68**, 1480 (1992).
[6] R. A. Lacey, A. Taranenko, N. N. Ajitanand, and J. M. Alexander, arXiv:1011. 6328v2.
[7] K. Geiger and B. Müller, Nucl. Phys. B **369**, 600 (1992).
[8] Zi-Wei Lin, Che Ming Ko, Bao-An li, Bin Zhang, and S. Pal, Phys. ReV. C **72**, 064901 (2005).
[9] Most recent references: Ben-Hao Sa, Dai-Mei Zhou, Bao-Guo Dong, Yu-Liang Yan, Hai-Liang Ma, and Xiao-Mei Li, J. Phys. G: Nucl. Part. Phys. **36**, 025007 (2009); Yu-Liang Yan, Dai-Mei Zhou, Bao-Guo Dong, Xiao-Mei Li, Hai-Liang Ma, and Ben-Hao Sa, Phys. ReV. C **79**, 054902 (2009).
[10] Zhe Xu and C. Greiner, Phys. Rev. C **71**, 064901 (2005).
[11] W. Cassing and E. L. Bratkovskaya, Nucl. Phys. A **831**, 215 (2009).
[12] B. Schenke, C. Gale, and S. Jeon, Phys. Rev. C **80**, 054913 (2009).
[13] T. Sjöstrand, Comput. Phys. Commun. **82**, 74 (1994).
[14] Ben-Hao Sa, Dai-Mei Zhou, and Zhi-Guang Tan, J. Phys. G: Nucl. Part. Phys. **32**, 0242 (2006); Dai-Mei Zhou, Xiao-Mei Li, Bao-Guo Dong, and Ben-Hao Sa, Phys. Lett. B **638**, 461 (2006); Yu-Liang Yan, Bao-Guo Dong, Dai-Mei Zhou,Xiao-Mei Li, Hai-Liang Ma, and Ben-Hao Sa, Phys. Lett. B **660**, 478 (2008); Xiao-Mei Li, Shou-Ping Li, Shou-Yang Hu, Dai-Mei Zhou, Zhi-Guang Tan, Feng Zhou, and Ben-Hao Sa, J. Phys. G: Nucl. Part. Phys. **34**, S873 (2007); Ben-Hao Sa, Dai-Mei Zhou, Yu-Liang Yan, Bao-Guo Dong, Hai-Liang Ma, and Xiao-Mei Li, Nucl. Phys. A **834**, 309c (2010); Dai-Mei Zhou, Ayut Limphirat, Yu-Liang Yan, Xiao-Mei Li, Yu-Peng Yan, and Ben-Hao Sa, Phys. Lett. B **694**, 435 (2011); Hai-Yan Long, Sheng-Qin Feng, Yu-Liang Yan, Dai-Mei Zhou, Hai-Liang Ma, and Ben-Hao Sa, arXiv:1103.2618v1.; Dai-Mei Zhou, Yu-Liang Yan, Bao-Guo Dong, Xiao-Mei Li, Du-Juan Wang, Xu Cai, and Ben-Hao Sa, to appear in Nucl. Phys. A.
[15] T. Sjöstrand, S. Mrenna, and P. Skands, J. High Energy Phys. **JHEP05**, 026 (2006).

[16] T. Sjöstrand, S. Mrenna, and P. Skands, Comput. Phys. Commun. **178**, 852 (2008).

[17] Ben-Hao Sa, A. Bonasera, An Tai, and Dai-Mei Zhou, Phys. Lett. B **537**, 268 (2002).

[18] B. I. Abelev, et al., STAR Collab., Phys. Rev. C **79**, 034909 (2009).

[19] Ben-Hao Sa and Tai An, Comput. Phys. Commun. **90**, 121 (1995); Tai An and Ben-Hao Sa, Comput. Phys. Commun. **116**, 353 (1999).

[20] R. Hagedorn, "Relativistic kinematics, a guide to the kinematic problems of high-energy physics", 1963, New York, Benjamin.

[21] Particle Data Group, "Particle Physics Booklet", 2010.

[22] P. Koch, B. Müller, and J. Rafelski Phys. Rep. **142**, 167 (1986).

[23] A. Baldini, et al., "Total cross sections for reactions of high energy particles", Springer-Verlag, Berlin, 1988.

[24] B. L. Combridge, J. Kripfgang, and J. Ranft, Phys. Lett. B **70**, 234 (1977).

[25] R. D. Field, "Applications of Perturbative QCD", 1989 by Addison-Wesley Publishing Company, Inc.

[26] B. Zhang, Comput. Phys. Commun. **109**, 193 (1998).

[27] J. Cugnon, T. Mizutani, and J. Vandermeulen, Nucl. Phys. A **352**, 505 (1981).

[28] ALICE Collaboration, arXiv:1012.3257v1.

[29] Tai An and Ben-Hao Sa, Phys. Lett. B **409**, 394 (1997).

[30] H. Pi, Comput. Phys. Commun., **71**, 173 (1992).

[31] B. Alver, et al, Phys. Rev. C **77**, 014906 (2008).

[32] K. Aamodt, et al., ALICE Collaboration, arXiv:1004.3514v1.

[33] K. Aamodt, et al., ALICE Collaboration, Eur. Phys. J. C **68**, 89 (2010).

[34] ALICE Collaboration, arXiv:1007.0719v2.

[35] ALICE Collaboration, arXiv:1012.1657v1.

[36] B. B. Back, et al., PHOBOS Collaboration, Phys. Lett. B **578**, 297 (2004).

[37] ALICE Collaboration, Phys. Lett. B **696**, 30 (2011).